Author Accepted Manuscript version of the paper by Njegos Jankovic et al.
in 2023 IEEE PES Innovative Smart Grid Technologies Conference Europe - ISGT-Europe (2023),
http://dx.doi.org/10.1109/ISGTEUROPE56780.2023.10408637

Decoupled Active and Reactive Power Controllers for Damping Low-Frequency Oscillations using Virtual Synchronous Machines

Njegos Jankovic
Electrical Systems Unit
IMDEA Energy Institute
Madrid, Spain
njegos.jankovic@imdea.org

Javier Roldán-Pérez
Electrical Systems Unit
IMDEA Energy Institute
Madrid, Spain
javier.roldan@imdea.org

Milan Prodanovic
Electrical Systems Unit
IMDEA Energy Institute
Madrid, Spain
milan.prodanovic@imdea.org

Salvatore D'Arco
Energy Systems
SINTEF Energy
Trondheim, Norway
salvatore.darco@sintef.no

Jon Are Suul
Energy Systems
SINTEF Energy
Trondheim, Norway
jon.a.suul@sintef.no

Luis Rouco
Institute for Research in Technology
ICAI, Comillas Pontifical University
Madrid, Spain
luis.rouco@iit.comillas.edu

***Abstract*—In this paper, a power oscillation damping (POD) controller embedded in virtual synchronous machines (VSMs) is proposed. This controller suggests the decoupled use of both active and reactive powers to damp low-frequency oscillations present in a power network. This allows for selecting either power component or both of them to damp the oscillations. This issue is relevant since transmission system operators are imposing new connection requirements to converter interfaced generators (CIGs) requesting grid-forming capability and POD. In the literature, it has been shown that these services can be provided using the VSM control technique. However, POD controllers are more complex in VSMs than in typical grid-following converters due to the inherent coupling between active and reactive powers. The performance of the proposed POD controller is evaluated by using electromagnetic transient simulations on a benchmark two-area power system with an additional CIG unit.**

I. Introduction

The ever-increasing penetration level of converter-interfaced generation (CIG) in electricity networks is having a significant impact on the system operation. This comes as a consequence of synchronous generators (SG) being decommissioned and replaced by CIGs [1]. With respect to the system stability, this fact is having a negative impact on frequency stability [2], voltage stability [3], as well as the small-signal rotor angle stability [4]. To address these issues, transmission system operators (TSOs) are imposing requirements for CIGs to provide additional services for supporting the network operation [5], [6].

The virtual synchronous machine (VSM) control approach tries to mimic the behaviour of SGs with CIGs [7]. This controller allows the active and reactive power responses of the CIG to be configured and adjusted. The VSM parameters can be set before the CIG commissioning or adjusted during the system operation, according to the network requirements [8], [9]. The power balance in the virtual swing equation of the VSM is responsible for providing frequency support by acting upon changes in the active power flow. Meanwhile, the reactive power controller is used to define the output voltage magnitude based on the changes in the reactive power flow.

The VSM controller directly affects the small-signal rotor angle stability of power networks [10]. When a VSM is connected to an existing power network, the VSM parameters can be set to avoid undesired small-signal interactions with the rest of the network [11]. Also, if the VSM is connected to a network that already has a poorly-damped low-frequency mode, additional control loops can be added to the VSM in order to help damping that mode [12]. Recent publications have proposed the use of adaptive virtual inertia [13] or multiple virtual swing equations for that purpose [14]. These works show the VSM can contribute to damping of the low-frequency oscillations by using either active or reactive power. However, the two power components are coupled and it is difficult to know beforehand the active and reactive powers required for the oscillation damping. The case of oscillation damping by active power is particularly to analyse for CIGs since it is directly linked to the primary source of energy.

The coupling between active and reactive powers is a natural phenomenon in power networks and depends on the system parameters and the network topology [15]. When a VSM is connected to a power network, this coupling is also affected by the internal parameters of the VSM. To avoid this coupling, a decoupling mechanism can be added to the control system. One approach is to add decoupling terms in the inner current control loop [16]. Another is to add additional terms to the virtual swing equation and the reactive power controller so that

This work is financially supported by the Spanish Government through the research project SOLARFLESS (TED2021-132854A-I00) and from Juan de la Cierva Incorporación program (IJC2019-042342-I). The work of Njegos Jankovic was supported by a Ph.D. Collaboration Agreement between Comillas Pontifical University and IMDEA Energy Institute

Author Accepted Manuscript version of the paper by Njegos Jankovic et al.
in 2023 IEEE PES Innovative Smart Grid Technologies Conference Europe - ISGT-Europe (2023),
http://dx.doi.org/10.1109/ISGTEUROPE56780.2023.10408637

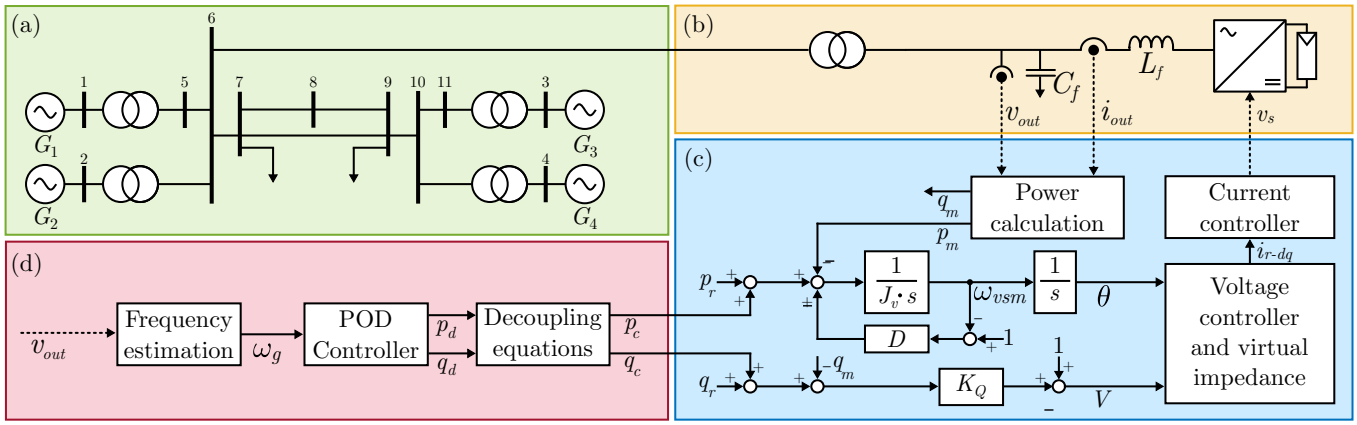

Fig. 1. (a) Single-line diagram of two-area power system, (b) CIG power-stage, (c) internal loops and VSM, and (d) proposed POD controller.

the voltage and angle generated by the VSM are modified [17]. These works show that it is possible to control active and reactive powers in a decoupled manner. However, the implementation of such mechanisms requires a modification of the internal control loops of the CIG, which may not be approved by the CIG manufacturer (and its intellectual property policy).

In this paper, a POD controller for VSMs that improves the damping of low-frequency modes present in a power network is proposed. This controller is based on conventional lead-lag filters plus a set of decoupling equations that define and allow the use of active and/or reactive power to damp the oscillations. Therefore, the proposed decoupling mechanism allows the CIG operator to select which power component should be used for oscillation damping and to set the margins accordingly. Also, there is no need to modify the internal loops of the CIG. The design procedure does not require an analytical model of the plant as it is based on system identification techniques. This makes this POD controller suitable for applications where a detailed small-signal model of the power system is not available. The proposed controller is tested in a two-area benchmark network where an additional CIG is connected.

II. System Overview

A. Application Description

Fig. 1 (a) shows the single-line diagram of the system studied in this work. It is based on the two-area benchmark network for low-frequency oscillation studies [18]. It consists of four generation units (G_{1-4}) that form two areas. Each generation unit includes a SG, a governor, an exciter and a power system stabiliser (PSS). There are two modifications compared to the model described in [18]. First, the proportional gain in each PSS has been reduced so that the inter-area mode is poorly damped. The second modification is an additional connection point in Bus 6 that is used to connect a CIG unit.

Fig. 1 (b) shows the CIG power stage. The primary energy source is connected to the dc side and it is modelled as an ideal dc voltage source that provides the required power. The primary source model is not considered here, but it is considered of interest for further research. The ac side of the power converter is connected to the rest of the system via an LC filter and a step-up transformer.

Fig. 1 (c) shows the block diagram of the internal loops and the VSM control algorithm. The inner current and voltage loops regulate the output current and voltage while the virtual impedance is used to simplify the integration with the rest of the network elements [19]. The voltage (V) and angle (θ) are references for the internal controllers by the VSM, and s is the Laplace variable. The definition of the VSM control algorithm and its parameters can be found in [11]. The values of the virtual impedance and VSM parameters (K_Q, J_V and D) are calculated according to the grid requirements [8].

Fig. 1 (d) shows the proposed POD controller. This controller acts on the estimated frequency of the grid (ω_g) and calculates the additional active and reactive power references that are used to damp oscillations (p_c and q_c, where c stands for "coupled"). The requirements for these two power components might vary depending on the available active power from the primary energy source and the converter ratings. Nonetheless, if applied directly, the power references would result in CIG delivering both power components as active and reactive powers are coupled. This poses an important problem because, if the power demanded to the primary source is larger than the available power, the CIG may collapse. For that reason, the implementation of a decoupling mechanism is of interest.

B. POD Controller Description

Fig. 2 (a) shows the block diagram of the POD controller. The frequency deviation ($\Delta\omega_g$) is used as the input signal for the POD controller (Δ stands for "incremental"). A high-pass filter ($H(s)$) is applied to eliminate the steady-state value of the frequency so that the controller only acts on frequency variations. Then, lead-lag compensators ($C_P(s)$ and $C_Q(s)$) are applied to compensate the open-loop phase of the plants while proportional gains (K_P and K_Q) are used to amplify the command signals [20].

Author Accepted Manuscript version of the paper by Njegos Jankovic et al.
in 2023 IEEE PES Innovative Smart Grid Technologies Conference Europe - ISGT-Europe (2023),
http://dx.doi.org/10.1109/ISGTEUROPE56780.2023.10408637

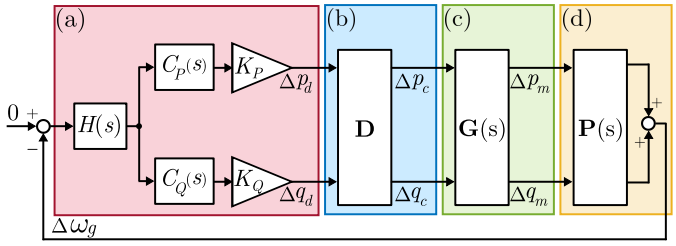

Fig. 2. (a) POD controller block diagram with (b) power decoupling mechanism and (c) dynamic model of the plant.

Fig. 2 (b) shows the decoupling system. This control block allows the operation with decoupled power references calculated by the POD controllers (p_d and q_d) applied to the original power references (p_c and q_c), that are coupled. This is done by multiplying p_d and q_d by a decoupling matrix ($\mathbf{D}$). The details and alternatives for the calculation of this decoupling matrix are explained in the following section. Fig. 2 (c) shows the inherent coupling $\boldsymbol{G(s)}$ between references and measured active and reactive powers. The injected active and reactive powers from CIG to the system have an effect on the system frequency. The dynamic relationships between these variables are summarised in $\boldsymbol{P(s)}$, shown in Fig. 2 (d).

III. Decoupling of Active and Reactive Powers

A. System Modelling

For a VSM connected to a power network, if any power reference is modified, the injection of both active and reactive power will change. This is not considered to be a problem, but rather a characteristic of the grid (e.g., by injecting active power both the voltage and the frequency change). If the system is operating in a steady state and only small disturbances are considered, the coupling between active and reactive power can be described as follows:

$$\begin{bmatrix}\Delta P_m(s)\\ \Delta Q_m(s)\end{bmatrix} = \underbrace{\begin{bmatrix}G_{PP}(s) & G_{PQ}(s)\\ G_{QP}(s) & G_{QQ}(s)\end{bmatrix}}_{\boldsymbol{G}(s)} \begin{bmatrix}\Delta P_c(s)\\ \Delta Q_c(s)\end{bmatrix}, \quad (1)$$

where $\boldsymbol{G}(s)$ represents the system dynamics and subindex m stands for "measured". Capital letters are used for signals and transfer functions in the Laplace domain. This system has a structure of a multiple-input multiple-output (MIMO) linear dynamic system [21]. The decoupling mechanism is designed to counteract coupling effect of the power components. It is defined as follows:

$$\begin{bmatrix}\Delta P_c(s)\\ \Delta Q_c(s)\end{bmatrix} = \mathbf{D} \begin{bmatrix}\Delta P_d(s)\\ \Delta Q_d(s)\end{bmatrix}, \quad (2)$$

where $\mathbf{D}$ is a 2×2 matrix.

B. Decoupling Options

The three most common methods to decouple MIMO systems are described in the following list [21]:

1) The first method is called *dynamic decoupling* and it allows to decouple each input-to-output response during both transients and in steady-state. To achieve such a requirement, the decoupling matrix is selected as follows:

$$\mathbf{D} = \hat{\mathbf{G}}^{-1}(s), \quad (3)$$

where $\hat{\mathbf{G}}(s)$ is a model of $\mathbf{G}(s)$. Even though this method is accurate, it has some important shortcomings. First, $\hat{\mathbf{G}}^{-1}(s)$ will have unstable poles if the original plant has right-hand place zeros. Also, $\hat{\mathbf{G}}^{-1}(s)$ usually has more zeros than poles, and therefore it cannot be easily implemented. The most common practical approach for addressing this is to multiply $\hat{\mathbf{G}}^{-1}(s)$ by additional high-frequency poles, but this increases the complexity and order of the system.
2) The second method is commonly called *decoupling at frequency* (e.g., ω_o) [21]. In this case, $\mathbf{D}$ is chosen to be exactly equal to $\hat{\mathbf{G}}^{-1}(s)$ at some specific frequency (ω_o). This can be written as follows:

$$\mathbf{D} = \hat{\mathbf{G}}^{-1}(j\omega_o). \quad (4)$$

Such decoupling mechanism would be of interest in poorly damped systems, where the frequency response is greatly affected by the frequency. This method is suitable for the application considered in this work. However, the main drawback is that $\mathbf{D}$ now consists of four complex numbers. Then, in order to implement this decoupling system, the complex multiplication would need to be implemented with additional filters (e.g., lead-lag filters).
3) The third method is called *steady-state decoupling* [21]. This method is a particular case of the one described in the previous point, but for $\omega_o = 0$:

$$\mathbf{D} = \hat{\mathbf{G}}^{-1}(0). \quad (5)$$

This selection decouples the response of the MIMO inputs and outputs, in steady state. The main benefit of this alternative is its simplicity, since $\mathbf{D}$ contains only real numbers. The coefficients of $\mathbf{D}$ can be readily calculated in real applications by applying step changes to the system inputs. Although the steady-state decoupling mechanism does not guarantee full decoupling during the transients, it contributes to the dynamic decoupling between the inputs as well [21]. This way of decoupling will be used in this work.

IV. Design of the POD Controller

A. Preliminaries

The design objective of the POD controller is to maximise the CIG damping action. To carry out the design, it is assumed that the power system is operating in steady state and that the linearised model is calculated. Then, the POD controllers for the active and the reactive powers are designed separately, as discussed in [22]. Only the design of the active power controller is described here since the procedure to design the reactive power controller is exactly the same.

Author Accepted Manuscript version of the paper by Njegos Jankovic et al.
in 2023 IEEE PES Innovative Smart Grid Technologies Conference Europe - ISGT-Europe (2023),
http://dx.doi.org/10.1109/ISGTEUROPE56780.2023.10408637

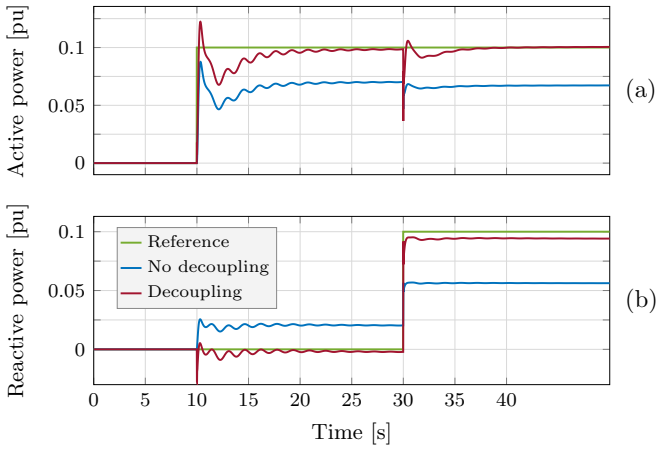

Fig. 3. Transient response of (a) active and (b) reactive powers after a step in the power references. (blue) Without and (red) with the decoupling mechanism.

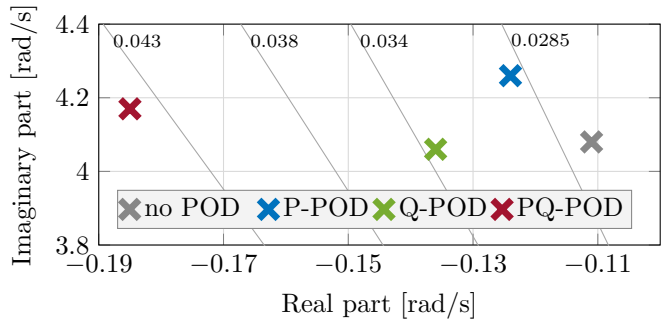

Fig. 4. Critical eigenvalue of the identified system for (gray) no POD, and POD with (blue) active, (green) reactive and (red) active and reactive power.

B. POD Controller Blocks

First, a high-pass filter is applied to the frequency so that the POD controller acts only over variations of $\Delta\omega_g$. It is defined as follows:

$$H(s) = s/(s + 1/T_h), \tag{6}$$

where T_h is the time constant of the filter.

The compensator $C_P(s)$ is designed following the open-loop phase compensation method [22]. First, the plant phase (ϕ_P) at the oscillation frequency (ω_o) is obtained. Then, the $C_P(s)$ is designed to compensate that phase at that frequency (see [20] for more details). The compensator $C_P(s)$ used for that purpose has the following structure:

$$C_P(s) = \frac{1 + sT_1}{1 + sT_2}, \tag{7}$$

where T_1 and T_2 are parameters of the lead-lag compensator.

The proportional gain (K_P) is designed in an iterative procedure where a compromise between the damping coefficient of the mode addressed and the negative impact on other modes should be considered. See [20] for more details. In addition, the power references are limited by saturations so that the CIG ratings are not exceeded [20].

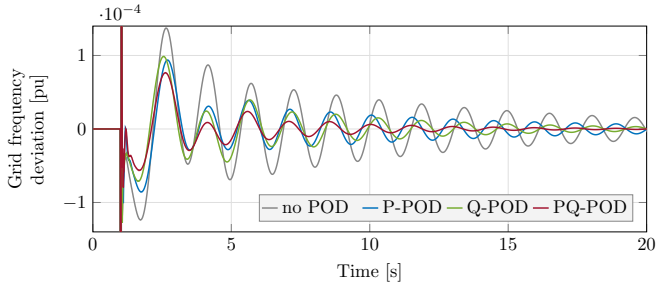

Fig. 5. Frequency deviation during the transient response (gray) without POD controller, and with POD controller based on (yellow) active power, (red) reactive power, and (green) both power components.

V. Numerical Results

A. Decoupling Power Components

Fig. 3 shows the transient response after changes applied to the active power reference (at $t = 10\ s$) and to the reactive power reference (at $t = 30\ s$). In blue, without decoupling, and in red, with the decoupling mechanism. For the case without decoupling equations, the steps are applied on p_r and q_r (i.e., the original power references). For the case with decoupling equations, the step changes are applied on p_d and q_d. These results show that the change of the active power reference causes a change of the reactive power, and vice versa. It can be seen that without the decoupling mechanism the coupling between power components is more pronounced. Moreover, it is removed in steady state. This result shows that this simple mechanism greatly helps to decouple power components.

B. Damping of Oscillatory Modes

Fig. 4 shows the critical system eigenvalues of the original system, and with the POD controller applied to active power, reactive power, and on both components. This eigenvalue has been obtained by using system identification techniques [23]. It can be seen that POD action by either (blue) active or (green) reactive power improves the damping of critical eigenvalue, compared to original network (in gray). Then, the combined action of both power components (red) results in a further improvement of the damping of the critical eigenvalue. This result shows that each of the POD controllers have a positive effect in the critical eigenvalue. Furthermore, thanks to the decoupling system, undesired interactions between control loops are avoided.

Fig. 5 shows the deviation of the estimated frequency (ω_g) after a disturbance, for four cases. The large frequency deviation in the first milliseconds is the result of electromagnetic transients and the response of the phase-locked loop (PLL) that is used to estimate the frequency. Then, the undamped low-frequency oscillation is the result of the interaction between the electrical areas. The action of either (blue) active or (green) reactive power improves the system damping and then the oscillations vanishes earlier. Then, the combined action of both power components (in red) further improves the transient response. These numerical results confirm the theoretical ones presented in Fig. 4.

Author Accepted Manuscript version of the paper by Njegos Jankovic et al.
in 2023 IEEE PES Innovative Smart Grid Technologies Conference Europe - ISGT-Europe (2023),
http://dx.doi.org/10.1109/ISGTEUROPE56780.2023.10408637

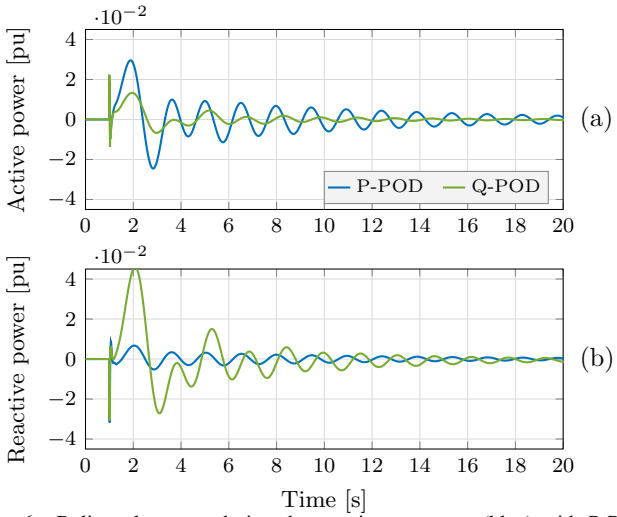

Fig. 6. Delivered powers during the transient response (blue) with P-POD controller, and (green) with Q-POD controller.

Fig. 6 shows the active and reactive powers injected during the frequency transients when only one component is used to damp oscillations. In Fig. 6 (a) (blue), it can be seen that the delivered active power is higher when active power is used to damp oscillations. However, there is also some reactive power injection in Fig. 6 (b) (blue). The similar issue happens when only the reactive power controller is applied (green curves). It should be noted that the injection of active and reactive powers during these transients is a result of the natural response of the VSM to variations in the grid frequency. This means that these oscillations are natural and cannot be avoided using the decoupling system implemented in the POD controller. These oscillations are of interest for further research.

VI. Conclusion

In this paper, a decoupled POD controller for low-frequency oscillation damping using CIGs has been proposed. The controller features an outer loop for CIGs operating as VSMs and can be deployed even if access to the CIG inner control loops is not available. The proposed POD controller is based on a steady-state decoupling mechanism and the traditional open-loop phase compensation technique. Only the open-loop phase of the plant at the frequency of the oscillation is required to design the controller. This makes the controller suitable for application in the cases when the full power system model is unavailable.

The presented results confirmed that the active and reactive powers being used to damp oscillations are successfully decoupled in steady state when the proposed decoupling strategy is applied. However, when an oscillation appears in the grid, some coupling is still present because of the natural response of the VSM. The results showed how the damping of the critical low-frequency mode was improved by using either active or reactive power. Also, it was shown that the combined use of active and reactive power further improves the system damping.

Future work will focus on developing a decoupling mechanism capable of acting not only in steady state but also during transients. Furthermore, the impact of the dc-side and the constraints on the primary source of energy will be considered.

References

[1] I. E. Agency, "Total primary energy supply by source, year and country," International Energy Agency, Tech. Rep., 2018.
[2] P. Tielens and D. Van Hertem, "The relevance of inertia in power systems," *Renewable and Sust. Energy Reviews*, vol. 55, pp. 999–1009, 2016.
[3] A. Adib, B. Mirafzal, X. Wang, and F. Blaabjerg, "On stability of voltage source inverters in weak grids," *IEEE Access*, vol. 6, pp. 4427–4439, 2018.
[4] R. Elliott, R. Byrne, A. Ellis, and L. Grant, "Impact of increased photovoltaic generation on inter-area oscillations in the western north american power system," in *2014 IEEE PES GM*, 2014, pp. 1–5.
[5] R. E. de España, *Technical norm of supervision on electrical generation modules according to EU Regulation 2016/631, (Spanish)*, 2019.
[6] T. N. Zealand, "Normal frequency management strategy," Transpower New Zealand, Tech. Rep., 2019.
[7] Q.-C. Zhong and G. Weiss, "Synchronverters: Inverters that mimic synchronous generators," *IEEE Trans. on Ind. Electronics*, vol. 58, no. 4, pp. 1259–1267, 2011.
[8] S. D'Arco, J. A. Suul, and O. B. Fosso, "Small-signal modeling and parametric sensitivity of a virtual synchronous machine in islanded operation," *Int. Journal of Elec. Power & Energy Systems*, vol. 72, pp. 3–15, 2015.
[9] J. Alipoor, Y. Miura, and T. Ise, "Power system stabilization using virtual synchronous generator with alternating moment of inertia," *IEEE Journal of Emerging and Selected Topics in Power Electronics*, vol. 3, no. 2, pp. 451–458, 2015.
[10] X. Zhou, S. Cheng, X. Wu, and X. Rao, "Influence of photovoltaic power plants based on vsg technology on low frequency oscillation of multi-machine power systems," *IEEE Trans. on Power Delivery*, vol. 37, no. 6, pp. 5376–5384, 2022.
[11] J. Roldán-Pérez, A. Rodríguez-Cabero, and M. Prodanovic, "Design and analysis of virtual synchronous machines in inductive and resistive weak grids," *IEEE Trans. on Energy Conv.*, vol. 34, no. 4, pp. 1818–1828, 2019.
[12] J. Roldán-Pérez, J. A. Suul, S. D'Arco, A. Rodríguez-Cabero, and M. Prodanovic, "Virtual synchronous machine control of vsc hvdc for power system oscillation damping," in *IECON 2018*, pp. 6026–6031.
[13] S. Fu, Y. Sun, Z. Liu, X. Hou, H. Han, and M. Su, "Power oscillation suppression in multi-vsg grid with adaptive virtual inertia," *Int. Journal of Elec. Power & Energy Systems*, vol. 135, p. 107472, 2022.
[14] N. B. Lai, L. Marín, A. Tarrasó, G. N. Baltas, and P. Rodriguez, "Frequency selective damping of sub-synchronous oscillations for grid-forming power converters," in *2021 IEEE ECCE*, 2021, pp. 877–881.
[15] P. Kundur, N. Balu, and M. Lauby, *Power system stability and control*, ser. EPRI power system engineering series. McGraw-Hill, 1994.
[16] M. Li, Y. Wang, N. Xu, W. Wang, Y. Liu, H. Wang, and Y. Weizheng, "A power decoupling control strategy for droop controlled inverters and virtual synchronous generators," in *2016 IEEE IPEMC-ECCE Asia*, 2016, pp. 1713–1719.
[17] T. Shintai, Y. Miura, and T. Ise, "Oscillation damping of a distributed generator using a virtual synchronous generator," *IEEE Transactions on Power Delivery*, vol. 29, no. 2, pp. 668–676, 2014.
[18] IEEE, "Benchmark systems for small-signal stability analysis and control," Tech. Rep., 2015.
[19] X. Wang, Y. W. Li, F. Blaabjerg, and P. C. Loh, "Virtual-impedance-based control for voltage-source and current-source converters," *IEEE Trans. on Power Elec.*, vol. 30, no. 12, pp. 7019–7037, 2015.
[20] N. Jankovic, J. Roldan-Perez, M. Prodanovic, J. A. Suul, S. D'Arco, and L. R. Rodriguez, "Power oscillation damping method suitable for network reconfigurations based on converter interfaced generation and combined use of active and reactive powers," *Intern. Journal of Elec. Power & En. Syst.*, vol. 149, p. 109010, 2023.
[21] S. Skogestad and I. Postlethwaite, *Multivariable Feedback Control: Analysis and Design*. Wiley, 1996.
[22] K. Ogata, *Modern control engineering*. Prentice hall, 2010.
[23] MATLAB. The MathWorks Inc., 2019.